35th Annual International Conference of the IEEE EMBS
Osaka, Japan, 3 - 7 July, 2013

Navigation Technique for MR-endoscope System Using A Wireless Accelerometer-based Remote Control Device *

Etsuko Kumamoto, *Member, IEEE*, Akihiro Takahashi, Yuichiro Matsuoka,
Yoshinori Morita, Hiromu Kutsumi, Takeshi Azuma and Kagayaki Kuroda, *Member, IEEE*

***Abstract*— The MR-endoscope system can perform magnetic resonance (MR) imaging during endoscopy and show the images obtained by using endoscope and MR. The MR-endoscope system can acquire a high-spatial resolution MR image with an intraluminal radiofrequency (RF) coil, and the navigation system shows the scope's location and orientation inside the human body and indicates MR images with a scope view. In order to conveniently perform an endoscopy and MR procedure, the design of the user interface is very important because it provides useful information. In this study, we propose a navigation system using a wireless accelerometer-based controller with Bluetooth technology and a navigation technique to set the intraluminal RF coil using the navigation system. The feasibility of using this wireless controller in the MR shield room was validated via phantom examinations of the influence on MR procedures and navigation accuracy. In vitro examinations using an isolated porcine stomach demonstrated the effectiveness of the navigation technique using a wireless remote-control device.**

I. Introduction

Recently, the development of an integrated MR-endoscope system that performs MR imaging during inspection and surgery with a flexible MR-conditional endoscope has been progressing[1][2][3]. Currently, advanced endoscopic therapy, such as endoscopic submucosal dissection (ESD), is performed for early-stage cancers. However, such a procedure requires a doctor with a high level of skill because the scope only views the surface of the gastric wall. The visualization of what is under the tissue surface is important for precise diagnosis and pre-operative planning. Compared with ultrasound imaging, MR images provide superior contrast in terms of the soft tissue structure inside the organ.

Therefore, we suggested an integrated MR-endoscope system with an intraluminal RF coil that could acquire a high-contrast image at a high resolution[4][5]. The MR compatible endoscope was used for setting and positioning the intraluminal coil in the gastric cavity. MR imaging using wide field of view (FOV) was applied to the position of the intraluminal coil in the body. Cubic substances, which saturated 5mM gadolinium contrast agent, were thoroughly covered with cling film and silicone to recognize the intraluminal coil. After detecting the intraluminal coil, anatomical structure imaging was applied. It took several minutes to detect the intraluminal coil and set the imaging conditions. The high-contrast MR image of the porcine gastric wall, which was acquired with an intraluminal RF coil, is shown in Figure 1. The layers of the gastric wall are clearly observable. The navigation software of the MR-endoscope system enables the system to show the scope's location and

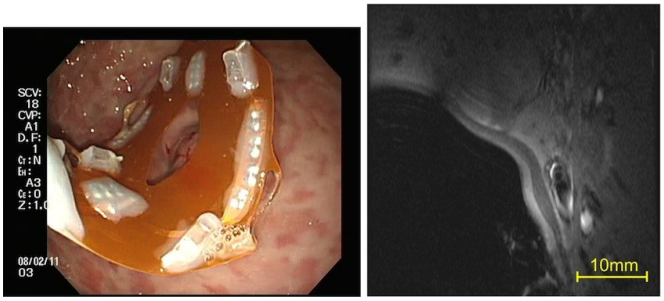

Figure 1 Intraluminal RF coil and MR image of the porcine gastric wall

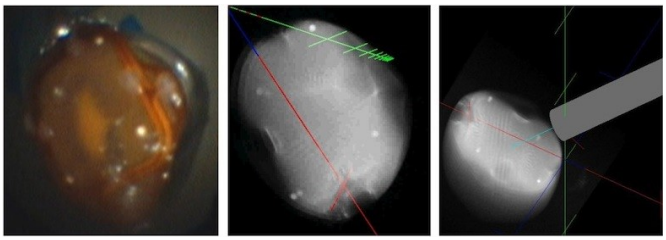

(a) (b) (c)

Figure 2 Synchronized kiwi images created by the navigation system. (a) Endoscopic view with the kiwi and intraluminal RF coil. (b) Endoscopic view image with MR volume data. (c) Bird's-eye view with MR volume data and the virtual endoscope object.

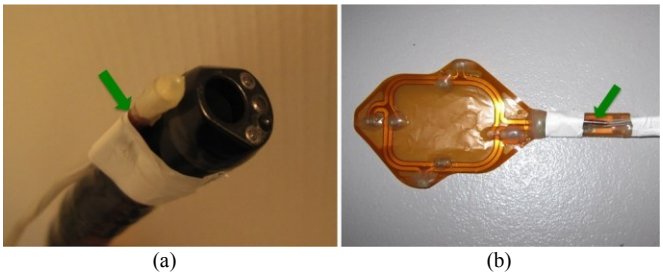

(a) (b)

Figure 3 Tracking sensor attached to the MR-compatible endoscope and intraluminal RF coil.

* This research is supported by grant number 24500547 from the JSPS Grant-in-Aid for Scientific Research (C).

E. Kumamoto is with the Information Science and Technology Center, Kobe University, 1-1 Rokkodai-cho, Nada, Kobe, Hyogo, Japan (e-mail: kumamoto@kobe-u.ac.jp).

A. Takahashi is with the Department of Systems Science, the Graduate School of Systems Informatics, Kobe University. Y. Matsuoka was with the Foundation for Kobe International Medical Alliance. Y. Matsuoka is now with the Center for Information and Neural Networks, National Institute of Information and Communications Technology and Osaka University. K. Kuroda is with the Foundation for Kobe International Medical Alliance and with Department of Human and Information Sciences, School of Information Science and Technology, Tokai University. Y. Morita, H. Kutsumi, and T. Azuma are with the Department of Internal Medicine, the Graduate School of Medicine, Kobe University.

orientation inside the human body in an MRI and to indicate the MR image with a scope view, as shown in Figure 2[6]. A tracking system based on a gradient magnetic field was used to obtain the location and orientation of the devices in the MR scanner. The tracking sensors were attached to an endoscope tip and the neck of the intraluminal RF coil, as shown in Figure 3. The examination with a dissected porcine stomach and a healthy swine had demonstrated the effectiveness of the prototype of the navigation software with the tracking system based on a gradient magnetic field[6][7]. The design of the user interface for the navigation system is very important because it must provide a great deal of useful, high-quality information for diagnosis and treatment. In this study, we proposed an MR-endoscope navigation system using a wireless accelerometer-based control device with Bluetooth technology and a navigation technique to set the intraluminal RF coil using the tracking system. The operating frequency of the Bluetooth signal (2.4 GHz) is far enough outside of the range of the MR signal. The feasibility of using Bluetooth technology to communicate with a host computer in an MR room with intense magnetic fields and electromagnetic waves is evaluated. The effectiveness of the navigation technique with a wireless control device is demonstrated via using an isolated porcine stomach.

II. MR-ENDOSCOPE NAVIGATION SYSTEM

An overview of the system configuration is shown in Figure 4. A 1.5T MR scanner (Signa EXCITE TwinSpeed, ver.11, GE Healthcare, USA) equipped with a tracking system (EndoScout, Robin Medical, Inc., USA) that detects the location and orientation in the MR scanner was used to develop the navigation system. The sensor of the tracking system, which was 6 mm in length and 1.5 mm in diameter, was attached to the tip of the MR-compatible endoscope (XGIF-MR30C, Olympus Medical Systems, Japan) and the neck of the intraluminal RF coil, as shown in Figure 3. The navigation software was developed on a navigator PC using the OpenGL graphical libraries. Bluetooth technology was used for communication with a wireless controller (WiiRemote, controller of Wii™, Nintendo Co., Ltd, Kyoto, Japan), as shown in Figure 5. A user interface module for the controller was based on the native WiiRemote C++ class library called "WiiYourSelf!" [8]. This software was designed to acquire DICOM format MR images and tracking system data though TCP/IP. The navigation system has the ability to zoom in/out, rotate, adjust window level (WL) and window width (WW), and show MR images selectively chosen from the MR volume data. Most of the functions were controlled with the wireless controller in the MR shield room.

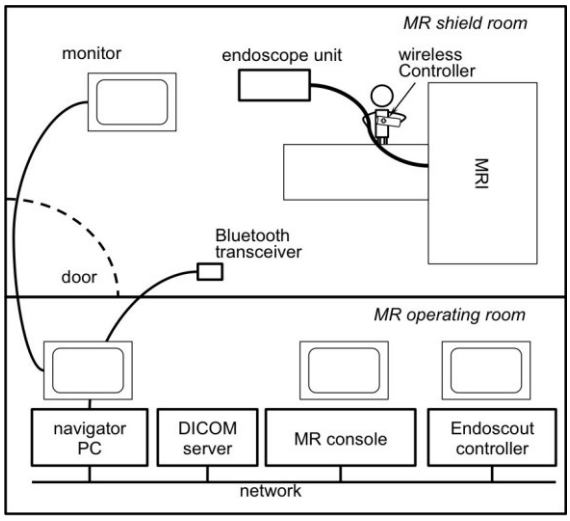

Figure 4 Overview of the MR-endoscope navigation system

Figure 5 The accelerometer-based wireless controller (WiiRemote)

III. BLUETOOTH COMMUNICATION IN MR ROOM

The wireless controller is equipped with some magnetic materials for use as a battery. However, the controller was not pulled by a magnetic field tens of centimeters away from the MR bore. The use of Bluetooth communication between the wireless controller in the MR shield room and the Navigator PC with a host adapter (PTM-UBT6, Princeton Technology, Ltd., Tokyo, Japan) was assessed for image quality and for the accuracy of the tracking data.

A. MR image quality

MR images of a spherical phantom filled with copper sulfate solution were acquired using three sequences and three conditions for the controller. The sequences were spoiled gradient recalled echoes in a steady state (SPGR) with the following conditions: TR = 200 ms, TE = 7 ms, field of view (FOV) = 24 x 24 cm^2, slice thickness = 5 mm, acquisition matrix = 256 x 128, and number of slices = 5. A spin echo (SE) with TR = 500 ms and TE = 12 ms, and a fast spin echo (FSE) with TR = 4000 ms, TE = 104 ms and echo train length = 16, were also used, with the other conditions being identical to those used with the SPGR. The conditions of the controller were C1: no controller in the MR shield room, C2: resting on the shelf in the MR shield room, and C3: swinging near the MR scanner (Figure 6). The acquired MR images are shown in Figure 7. No noise or image deterioration was detected in the MR images. The signal-to-noise ratios (SNRs) of the images were calculated by using the standard deviation of the air background[9].

$$SNR = S / N \quad (1)$$

where S is the mean pixel value within the ROI on the phantom area and N is the standard deviation of the pixel values within the ROI on the background. The ROI on the phantom area was 20.1 mm x 20.1 mm square, and the ROI on the background area for the noise image was a 20.5 mm x 20.3 mm square. Figure 8 shows the average SNRs (n=5). The error

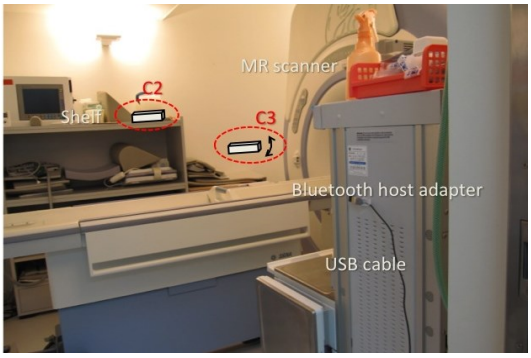

Figure 6 Experimental conditions in the MR shield room.

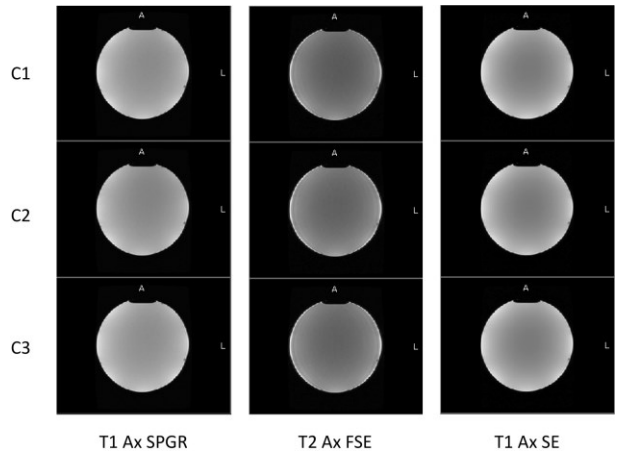

Figure 7 MR images of the spherical phantom

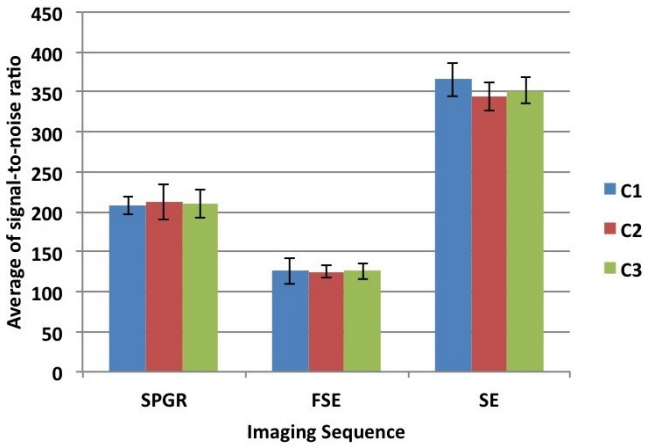

Figure 8 Average signal-to-noise ratios

bar shows the standard deviation. With the use of a two-tailed Welch's t-test for paired conditions (between C1 and C2, C1 and C3, $t(8)=2.306$, $p < 0.05$), there was no significant difference in the means of the SNRs. There was no effect on MR images from Bluetooth communication between the controller inside the MR shield room and the PC.

B. Tracking data accuracy

The influence of Bluetooth communication on the tracking system was then examined under the C1-C3 conditions. The tracking sensor was placed at the P1-P3 positions, which are shown in Figure 9. The two hundred location data points (x_i, y_i, z_i) of the tracking sensor were acquired at intervals of 63 milliseconds. The average of the location data (x, y, z) was calculated in order to evaluate tracking accuracy. The distances between the locations under C1 and other conditions are shown in Table 1. The maximum error was 0.89 mm. This was observed at location P3 when the controller was on the shelf. The errors were smaller than 0.18 mm, except at location P3. From this, it can be shown that inadequate fixing of the sensor is capable of causing maximum error. Bluetooth communication between the controller inside the MR shield room and the PC has no effect on tracking accuracy.

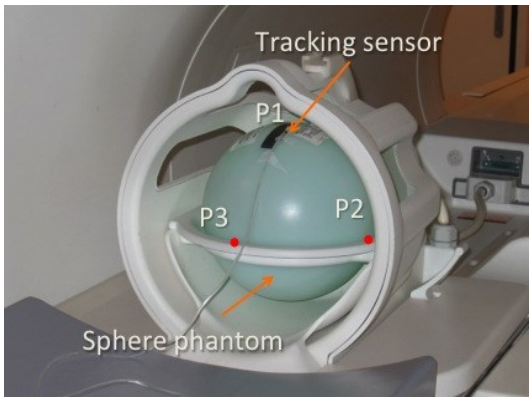

Figure 9 Location of the tracking sensors on the spherical phantom

Table 1 Error between C2/C3 and C1 [mm]

	C2				C3			
	x	y	z	Euclidean	x	y	z	Euclidean
P1	0.028	0.094	0.100	0.140	0.030	0.002	0.080	0.085
P2	0.081	0.030	0.156	0.178	0.116	0.057	0.076	0.150
P3	0.372	0.802	0.079	0.888	0.109	0.893	0.072	0.902

IV. Navigation Experience in Vitro

An in vitro experiment using a dissected porcine stomach with the esophagus was performed. First, MR volume images with a large field of view (FOV) (30 x 30 cm^2) were obtained using the body coil on a T2-weighted fast-spin echo (T2FSE). Second, the coordinate of the center of the intraluminal RF coil was saved by moving the tip of the endoscope close to the setting position and clicking the "A" button on the controller. The position of the intraluminal coil was drawn as a red point on the MR volume data, as shown in Figure 10. Next, the intraluminal RF coil was placed at the setting point on the gastric mucosa. The straight-line path from the RF coil to the setting position was drawn with a blue line, as shown in Figure 11. The color of the line changed to green when the RF coil approached the setting point. The coordinate of this point should also be considered the image center for MR imaging when using the intraluminal RF coil. The MR scan was conducted with the T2FSE, TR = 3000 ms, TE = 105.7 ms, ET = 18, RBW = 122.1 KHz, slice thickness = 3.0 mm, slice gap = 0.0 mm, FOV = 6 x 6 cm^2, acquisition matrix = 256 x 256 and number of slices = 11. The high-spatial resolution MR volume data obtained by using the intraluminal coil is shown

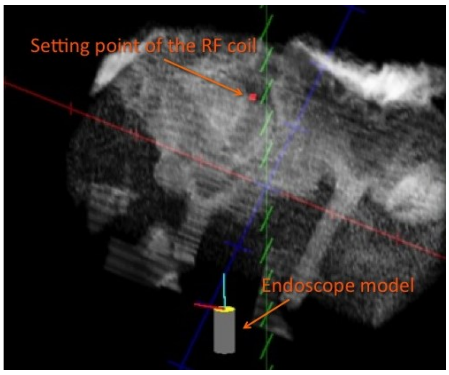

Figure 10 Setting point of the intraluminal RF coil on the MR volume data of the porcine stomach.

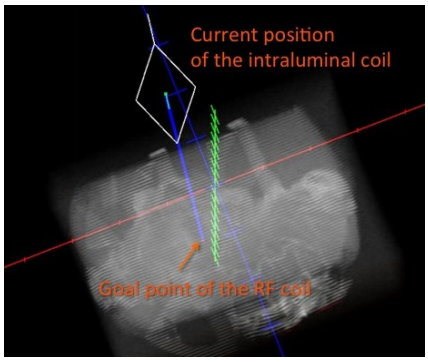

Figure 11 Model of the intraluminal RF coil and the setting position.

in Figure 12, and the MR image chosen from the MR volume data can be shown in a pop-up view (Figure 13).

The experiment demonstrated that it is no longer necessary for MR imaging to detect the intraluminal coil and it is possible to set up an intraluminal RF coil and execute an MR procedure quickly with our proposed navigation system.

V. Conclusion

No significant signal-to-noise ratio reduction was found due to operating the wireless control device near the magnet in the MR shield room. Although a slight error in the location estimation was observed for the gradient field sensor, the performance of the tracking system was not affected by the wireless controller equipment. This indicates that the use of a wireless controller in an interventional MR suite is possible. The resultant MR procedure, with navigation software using the wireless controller, was also successful, as indicated by the fact that the image manipulation obviously became smooth and intuitive in comparison with mouse/keyboard operation. Furthermore, the setup operation of the RF intraluminal coil and the MR imaging procedure became quicker than the procedure without navigation software. In real condition, the movement and the deformation of the abdomen will introduce inconsistency of the information constructed by the navigation system. In future research, we will sophisticate the MR-endoscope navigation system to adapt the movement and deformation of the organs, and will examine the feasibility of our system via an in vivo animal experiment.

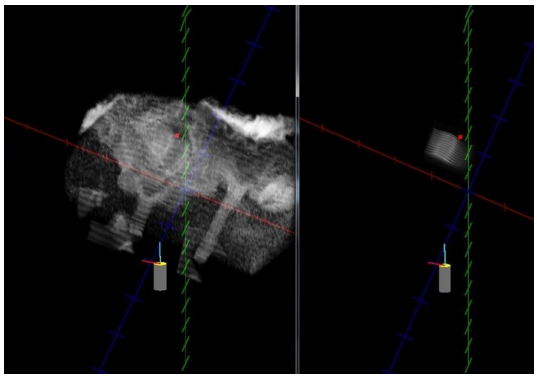

Figure 12 The MR volume images acquired with the body coil and the intraluminal RF coil.

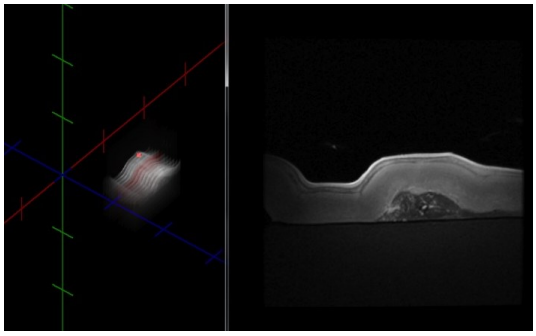

Figure 13 The MR volume images and selectively chosen MR image acquired with the intraluminal RF coil.

References

[1] K. Inui, S. Nakazawa, J. Yoshino and H. Ukai, Endoscopic MRI, *Pancreas*. Vol.16, No.3, pp.413-7, 1998.

[2] D. J. Gilderdale, A. D. Williams, U. Dave and N. M. deSouza, An inductively-coupled detachable receiver coil system for use with magnetic resonance compatible endoscopes. *J Magn Reson Imaging*, Vol. 18, No. 1, pp.131-5, 2003.

[3] Y. Matsuoka, K. Kuroda, E. Kumamoto, A. Saito, T. Mine, T. Shibasaki, and B. Keserci, An integrated MR-endoscope for diagnosis of luminal organ, *Proc 12th Int Soc. Mag. Reson. Med.*, pp.969, 2004.

[4] H. Yoshinaka, Y. Morita, Y. Matsuoka, D. Obata, S. Fujiwara, R. Chinzei, M. Sugimoto, T. Sanuki, M. Yoshida, H. Inokuchi, E. Kumamoto, K. Kuroda, T. Azuma and H. Kutsumi, Endoluminal MR imaging of porcine gastric structure in vivo, *J Gastroenterol.*, Vol.45, No. 6, pp.600-7, 2010.

[5] Y. Matsuoka, Y. Morita, H. Kutsumi, H. Miyasho, M. Matsumoto, T. Miyamoto, E. Kumamoto, T. Azuma, and K. Kuroda, Imaging of Anatomical Structure and Blood Vessels in Porcine Gastric Wall by MR Endoscope, *Proc 16th Int Soc. Mag. Reson. Med.*, pp.278, 2008.

[6] S. Aizawa, M. Matsumoto, Y. Matsuoka, K. Kuroda and E. Kumamoto, Development of visualization software for MR-endoscope tracked by a magnetic field sensor, *Proc. 8th Interventional MRI Symposium*, pp. 288-290, 2010.

[7] Y. Matsuoka, A. Takahashi, E. Kumamoto, Y. Morita, M. Takenaka, A. Sakai, H. Kutsumi, T. Azuma and K. Kuroda, Navigation for adequate MR scan with integrated MR-endoscope system using intraluminal RF coil, *Proc. 9th Interventional MRI Symposium*, pp. 143, 2012.

[8] WiiYourself! gl.tter's native C++ WiiRemote library, http://wiiyourself.gl.tter.org/ (accessed on Nov. 10th, 2012).

[9] National Electrical Manufacturers Association, Determination of Signal-Noise Ratio (SNR) in Diagnostic Magnetic Resonance Images. *NEMA Standard Publications*, MS 1-2008, 2008.